ELSEVIER

Ceramics International 28 (2002) 719–729

CERAMICS INTERNATIONAL

www.elsevier.com/locate/ceramint

Easy-to-use mullite and spinel sols as bonding agents in a high-alumina based ultra low cement castable

S. Mukhopadhyay*, S. Ghosh, M.K. Mahapatra, R. Mazumder, P. Barick, S. Gupta, S. Chakraborty

College of Ceramic Technology, 73 A. C. Banerjee Lane, Kolkata 700 010, India

Received 19 October 2001; received in revised form 28 November 2001; accepted 7 February 2002

Abstract

This paper deals with the preparation of colloidal suspensions of mullite and magnesium-aluminate spinel via a cheaper precursor of alumina sol. Viscosity, pH, solid content, DTA, TGA and XRD studies at different temperatures were performed to characterize those two sols. These mullite and spinel sols were used separately as bonding agents in a high-alumina based ultra low cement castable composition prepared by simple tapping technique and their performances have been compared in terms of bulk density, apparent porosity, cold crushing strength, flexural strength, slag corrosion, thermal shock, XRD and SEM reports. The results confirm that the mullite sol excels while the spinel sol degrades the refractory castable quality.

Keywords: D. Mullite; D. Spinel; Sols; Bonding agents; High alumina castables

1. Introduction

Castables have been progressively gaining market share in all areas of refractory application in both ferrous and non-ferrous industries, replacing conventional concretes and ramming mixes [1, 2]. Mullite and magnesium-aluminate spinel are very much desirable phases in castables where improved hot strength, creep resistance, good thermal stability and slag penetration resistance are required. A wide variety of self-flow, no-cement and ultra low cement castables have been addressed by several authors [3], and colloidal stability software has also been developed to evaluate the castable properties [4].

Nowadays, a new bonding agent with superfine materials prepared from sol-gel route, appeared in the industry, which opened a new horizon for refractory technologists. The principle behind this bonding is formation of gel from a sol that surrounds the refractory aggregates and binds them through a network skeleton. It also reduces cement, and on subsequent heating develops strength via ceramic bonding by low temperature sintering and upgrades its high temperature properties [5]. These sol-gel binders differ from bulk sol-gel products because they only serve as bonding systems rather than the main body. Silica and alumina sols have been tried in this purpose although a huge literature information is not available. For alumina ceramics, boehmite has been suggested to be a binder and boehmite sol as a dispersant and the fabrication of several kinds of alumina products, as found in some literatures [6–10], is based on the use of this boehmite precursor. Mullite and mag–al spinel gels have been synthesized by several workers [11,12] and found to be dependent on the intimacy of mixing of the respective ingredients. Starting from a cost effective boehmite sol precursor, mullite and spinel bonds can be conveniently prepared within the matrix of castables and as such a new generation of binders could be identified which are water compatible, inexpensive and capable to form low temperature bonding.

In this present investigation, an attempt has been made to synthesize the colloidal suspensions of mullite and mag–al spinel from a cheaper precursor like boehmite sol and the sols have been characterized with respect to viscosity, pH, solid content, DTA, TGA and XRD studies at different temperatures. These two sols were separately used as bonding agents to a tabular and fused alumina based ultra low cement castable composition

* Corresponding author.
E-mail address: msunanda_cct@yahoo.com (S. Mukhopadhyay).

0272-8842/02/$22.00
PII: S0272-8842(02)00034-2

and the samples were prepared by simple tapping method without vibration. A comparative study was done between these two kinds of sol-bonded castables with respect to bulk density, apparent porosity, cold crushing strength, flexural strength, thermal shock and slag corrosion resistance. X-ray diffraction analysis and scanning electron microscope studies of some fired samples were carried out to compare the effect of those sols on the physico-mechanical properties of castables.

2. Experimental

Alumina (boehmite) sol, prepared from the ammonia-nitrate route [13], having pH vale 2–4, particle size 14 nm and solid content about 5% was taken as the precursor material. Its viscosity, DTA, XRD, etc. have been reported [13]. To this boehmite sol, silica fume (CAB-O-SIL Fumed Silica, Cabot Corporation, USA, grade M-5, particle size 0.014 μm, S. A. = 200 m^2/gm) and $MgCl_2{\cdot}6H_2O$ (NEDMAG Industries) were slowly added in requisite amount with vigorous stirring (Fig. 1) to prepare mullite and mag–al spinel colloidal suspension or sols respectively, maintaining the stoichiometries of the said compounds during mixing [11,14,15]. Both the sols were characterized with respect to viscosity, pH and solid content. DTA, TGA and XRD at different temperatures (with 2 h of soaking) were also done with the sol powders dried at ambient temperature.

Viscosity measurement at room temperature was conducted by using a HAAKE Viscometer (model VT-500). X-ray diffraction patterns were taken from a SCINTAG XRD instrument with Ni-filtered CuK_α (USA). DTA and TGA studies were carried at a rate of 10 °C/min in NETZSCH (Gerateban GmbHS) instrument, model no. STA-409C.

In the second phase of experiment the effect of sols were compared. The batch composition (Table 1) was used to prepare the ultra low cement castable (ULCC) specimens after being added separately with mullite and mag–al spinel sols instead of water.

The sol-bonded ULCC samples were named as M and S respectively to distinguish the two sols. The samples were cast by simple tapping technique with cube (25.4 mm) and bar (75×12.5×12.5 mm)-type moulds to improve particle-packing [16]. All of these specimens were then cured under humid conditions for 24 h followed by 24 h of air drying and oven drying at 110 °C. Finally the samples were fired at various temperatures (900, 1200, 1500 °C) with 2 h. of soaking time. To get a clear comparative study of two sols, the fired castables specimens were subjected to various tests such as bulk density (BD), apparent porosity (AP), cold crushing

Table 1
Batch composition of castable using presently prepared sols

Batch material	Wt.%
Aggregates (tabular and fused alumina, coarse, medium and fine)	72
Microsilica	5.5
Sillimanite sand	7
Microfine alumina	
Grade 1	7
Grade 2	7
Calcium aluminate cement	1.5
Deflocculant	0.05% of the total batch
Sol (any one)	Vol./wt.%
Mullite	10%
Spinel	13%

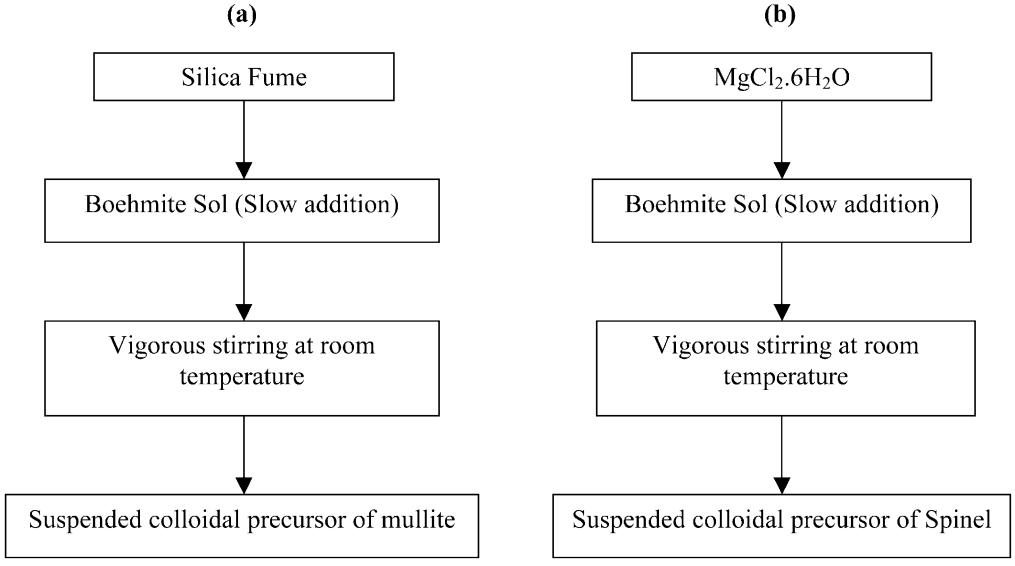

Fig. 1. Flow chart for the preparation of sols from boehmite precursor: (a) mullite, (b) mag–al spinel sol.

strength (CCS), thermal shock resistance, slag corrosion resistance at elevated temperature and flexural strength at room temperature. BD, AP and CCS were done by standard test methods. With 1200 °C fired samples, XRD and SEM tests were also performed to emphasize the effect of sols. The flexural strength of M and S type bars (previously fired at 1500 °C) was conducted with an Universal Testing Machine INSTRON-1185 at 25 °C with a cross head speed 0.5 mm/min and a span of 50 mm. The thermal shock resistance (spalling test) of M and S specimens, previously fired at 1500 °C, were noted in terms of residual strength after 5 cycles of thermal shock, each cycle was completed by putting the fired samples in a furnace at 800 °C for 10 min followed by immersing them in water at room temperature for another 10 min. For the slag corrosion test, cubes of 25 mm were cast, cured for 24 h, dried at 110 °C followed by heat treatment at 1200 °C for 2 h. A cylindrical void of the same size was made at the middle in all the cubes.

The void (groove) was filled up with slag (TISCO, India, given in Table 2) and the cube was heated at 1600 °C for 2 h. After cooling, the sample was cut across the middle and the extent of slag penetration was studied. The SEM study of a few ULCC fired samples was done in the instrument Hitachi S-2300. The comparative study of the results of all these experiments were carried out to interpret the differences of interaction of these two sols in the ULCC matrix.

Table 2
Chemical composition of slag

Ingredients	Wt.%
SiO_2	33.74
CaO	32.27
Al_2O_3	18.98
MgO	9.88

3. Results and discussion

3.1. Characteristics of the prepared sols

3.1.1. Viscosity

Fig. 2(a) and (b) show the viscosity vs. shear rate curves for mullite and mag–al spinel sols, respectively,

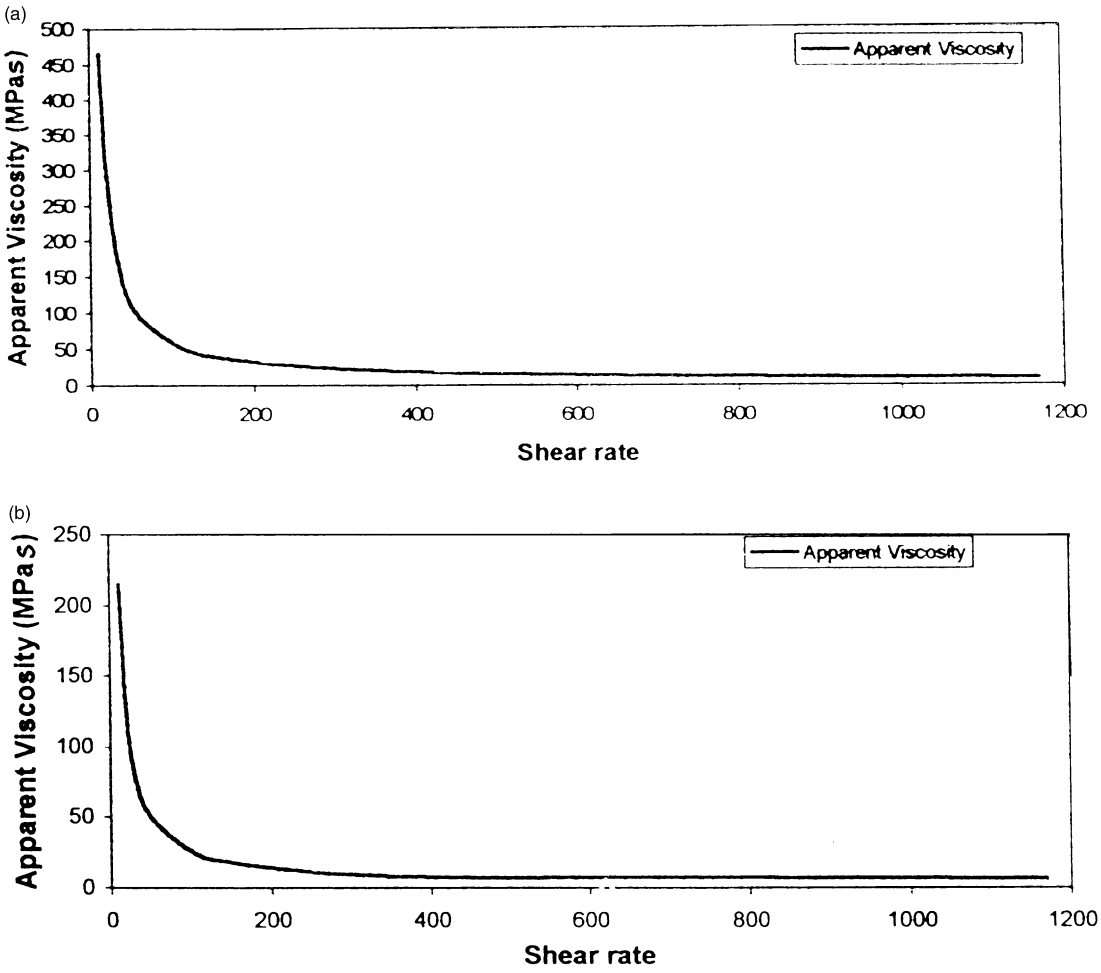

Fig. 2. Variation of apparent viscosity with shear rate of sols: (a) mullite, (b) mag–al spinel sol.

and both of them indicate the same pseudoplastic nature. We may say therefore, more efficient particle packing reduces the range of sizes of interstices among particle [17] and the sols possess enough fluidity, which may help in casting the ULCC samples.

3.1.2. Solid content

The solid content was determined by the well-known ignition method and found to be 6 and 5%, respectively, for mullite and mag–al spinel sols.

3.1.3. pH value

For both the sols, this value was within the range of 3–4.

3.1.4. DTA and TGA

A number of factors influence the chemical reactions for mullite formation which include particle size and crystalline forms of precursors, Al/Si ratio, degree of mixing and impurities present in samples [18,19]. During the crystallization process and the formation of Al–O–Si bond, the processing conditions and the sources of different components of silica and alumina may affect the variation in thermal sequence of changes in monophasic and diphasic gel systems [20–27]. TGA and DTA reports of mullite sol, [Fig. 3(a) and (b)] show the weight loss due to the release of free water and bonded OH groups. The small exotherm reaction around 380 °C may be due to the loss of some adhered nitrate compound. The absence of any significant weight-change after this indicates the onset of crystallization. The peak around 600 °C can be due to the dehydration of boehmite in concurrence with the rapid crystallization of Si–Al spinel phase which is promoted due to the intimate mixing of the components on a colloidal scale. The decrease in the rate of weight-loss is nearly completed at 900 °C. The small exotherm reaction at around 1040 °C may be associated with the appearance of a minor amount of cubic or tetragonal mullite [23] that forms further at 1200 °C, and which in due course of heating around 1240 °C, is converted to orthorhombic mullite [21]. Many other researchers suggested the solid state reaction between intermediate γ or δ or θ-Al_2O_3 with β-cristobalite or amorphous silica, to be responsible for mullite formation.

The low temperature synthesis of mag–al spinel and the thermal and other behavior related to this have been investigated by a lot of researchers [28–35]. The DTA and TGA reports of the mag–al spinel sol [Fig. 4(a) and (b)] show that the endothermic peak found at around 960 °C suggests the spinellisation process takes place quite earlier, in comparison with the solid state reaction between pure oxides. It is also observed that the weight-loss continues up to 600 °C suggesting that the dehydration and the dechlorination processes continue up to that temperature. We know that when heated, hydrated magnesium chloride melts first and then undergoes hydrolysis above 185 °C giving off steam, HCl and magnesium oxychloride (Mg_2OCl_2). This on further heating in oxygen of the air, decomposes to produce magnesium oxide and chlorine as shown below,

$$2\ MgCl_2 \cdot 6\ H_2O = Mg_2OCl_2 + 11\ H_2O + 2\ HCl$$

$$2\ Mg_2OCl_2 + O_2 = 4\ MgO + 2\ Cl_2$$

Thus the peak immediately around 300 and 400 °C may probably be due to the decomposition of chloride present and formation of γ-alumina phase, respectively.

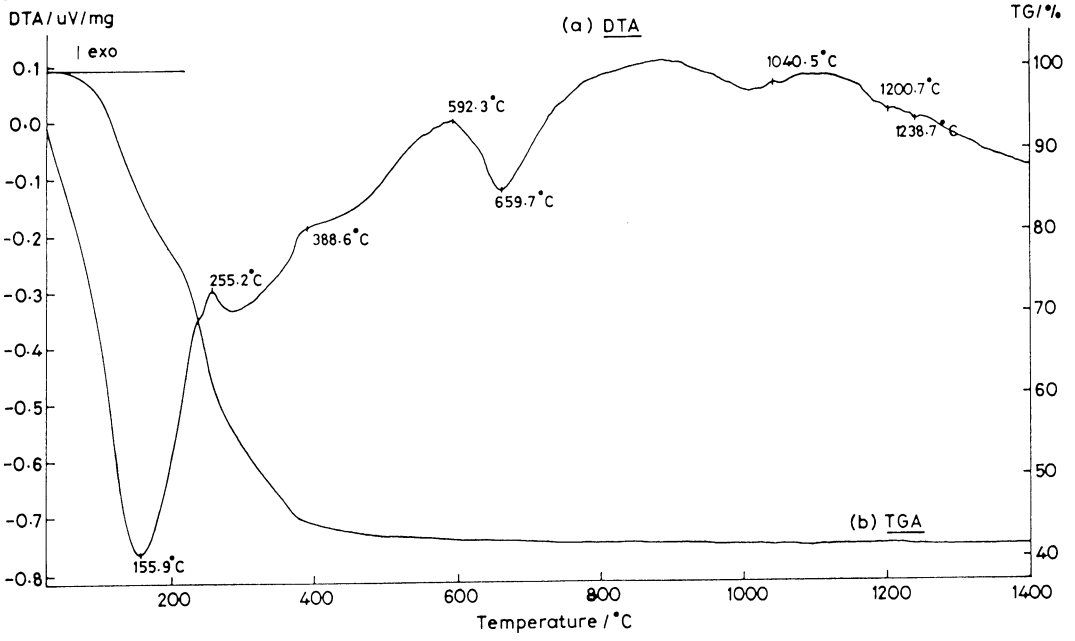

Fig. 3. (a) DTA and (b) TGA patterns of mullite sol.

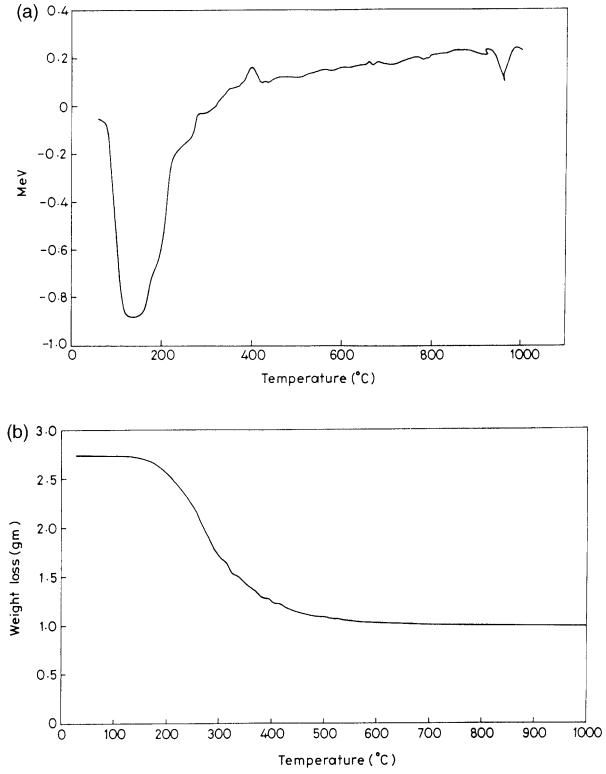

Fig. 4. (a) DTA and (b) TGA patterns of mag–al spinel sol.

3.1.5. XRD pattern

Fig. 5(a) shows that increased amount of mullite has been formed in the heated powder of mullite sol (soaked for 2 h) between 1000 and 1200 °C as corroborated from the DTA report discussed earlier. Fig. 5(b) shows that when the spinel sol-powder was heated at different temperatures, spinel phase has been formed quite earlier at 450 °C and developed in due course with increasing temperature.

3.2. Properties of sol bonded castables and their comparison

3.2.1. BD, AP and CCS

The variation of bulk density, apparent porosity and cold crushing strength of the ULCC samples heated at various temperatures are illustrated in Fig. 6(a–c), respectively. S and M code names were used respectively for ULCC castable bonded with mag–al spinel and mullite sols. All those figures indicate that mullite sol performs quite better than the other. However at 110 °C, both the samples show very poor green strength [Fig. 6(c)] which is very common with ultra low cement compositions. The rheology of both the sols indicate their pseudoplastic nature which may help in casting the samples by eliminating expensive technique (e.g. vibration) and enhancing the flowability of castable. We know, to have a satisfactory free-flow, the system has to be well dispersed and friction between particles to be

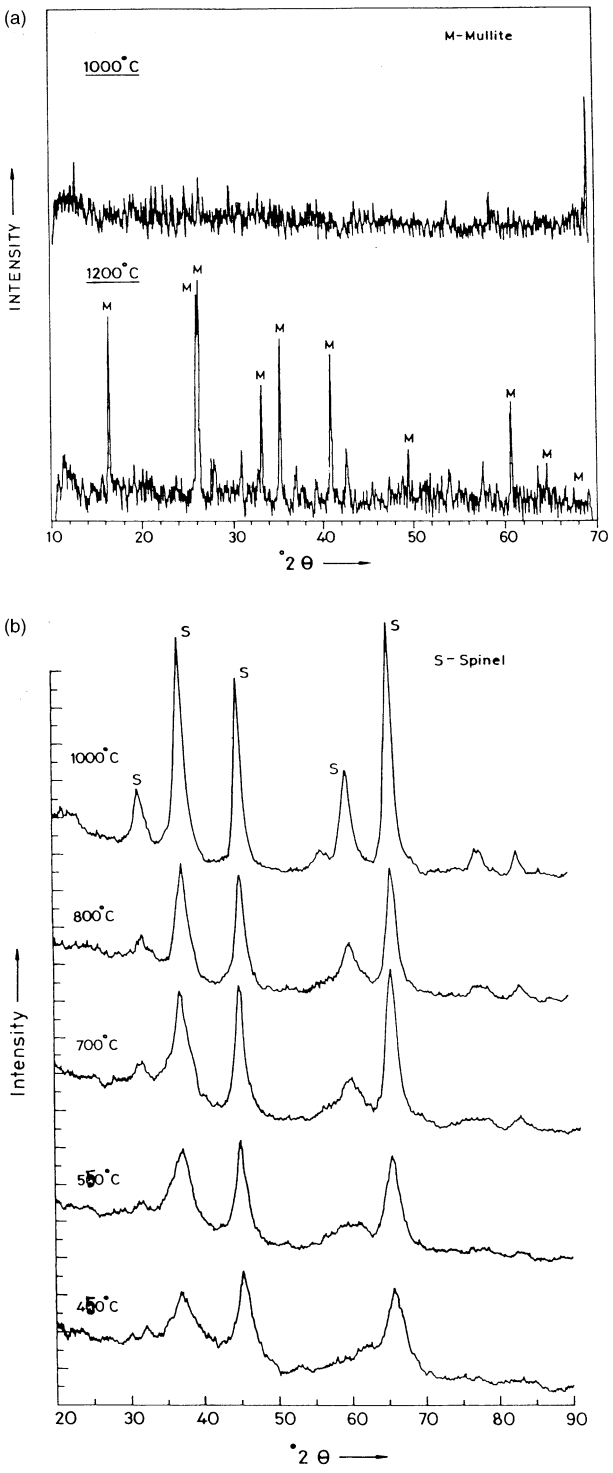

Fig. 5. (a) XRD patterns of heated mullite sol powder at 1000 and 1200 °C (M = mullite). (b) XRD patterns of heated mag–al spinel sol powder at 450, 550, 700, 800 and 1000 °C (S = spinel).

minimized. Mullite sol satisfies these criteria more efficiently, because in these M-bonded castables, the sol (amount = 10%) gives a coating to the coarse refractory grain surface, fills the voids among them and accomplishes the separation between aggregates. But for mag–al sol, the amount is greater (13%) and its solid content

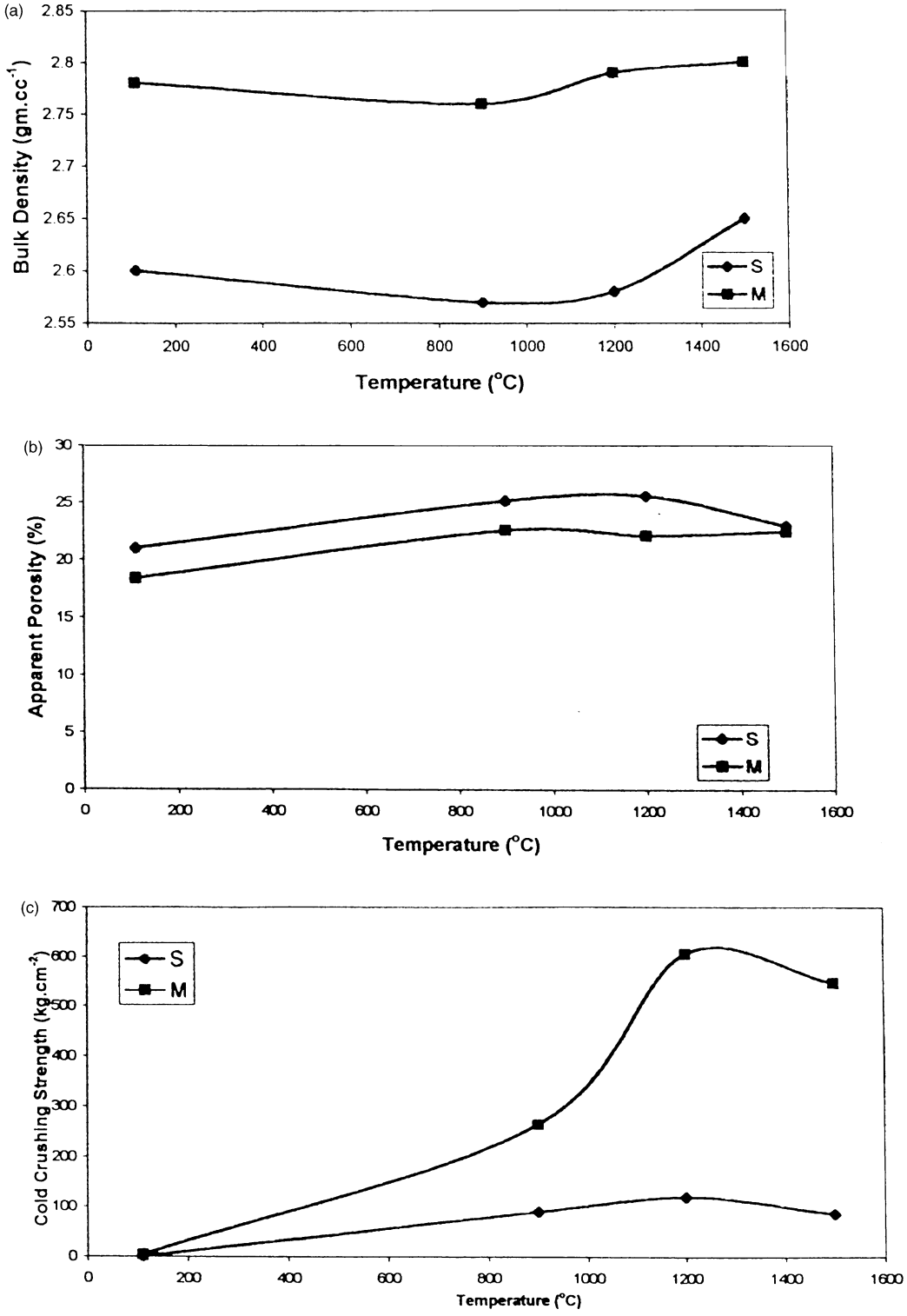

Fig. 6. Physical properties of M and S type ultra low cement castable in relation to heating temperatures: (a) bulk density, (b) apparent porosity and (c) cold crushing strength.

(5%) is less than the mullite sol (6%). Therefore during the mixing of S-samples, the aggregate particles that are supposed to be at a relatively fixed distance to each other, get separated by the extra film of liquid and the density is automatically reduced from the very beginning. Poor bulk density and more porosity in S-samples as observed from [Fig. 6(a) and (b)], may be due to this loose compaction, loss of adhesion of adjacent matrices and break in the continuity of their texture. The quality of S-samples deteriorated with respect to M-ones also at

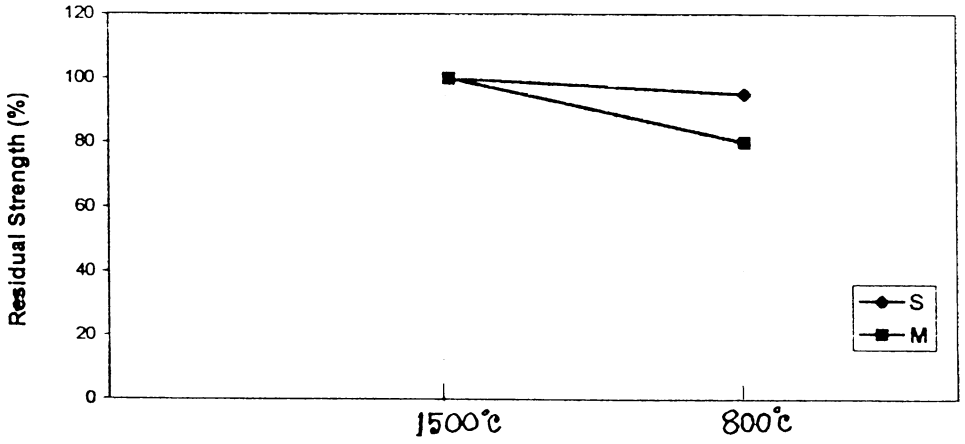

Fig. 7. Percentage residual strength of M and S type castable specimens.

elevated temperatures. The DTA report of spinel sol shows that its pyrolysis occurs for an extended period and a significant weight loss takes place due to the presence of chloride. It is also known that the process of crystal growth of refractory oxide in an atmosphere containing hydrogen chloride is considerably faster than in a normal furnace atmosphere. This is corroborated from the XRD-reports which show that spinellisation occurs at as low as 450 °C. Hence, the formation of spinel in S-samples is associated with a considerable volume expansion (5%) [36] and results in the bursting of the product. As mentioned earlier, during the extended pyrolysis period of S-bonded castables, gas inclusions may be entrapped within the matrix, which may produce sporadic larger flaws in the long run. Apart from this, by taking iron oxide (whatever small coming from moulds during casting) into solid solution, an inverted ferrite spinel may form, which upon alloying with the normal spinel, also causes the expansion in volume.

The tendency of decrease in BD and increase in AP up to 900 °C for both M and S-type samples may happen due to the dehydration of high alumina cement as usually happens in castables. The quality of M-samples at higher temperatures increases manifold than S ones [Fig. 6(c)]. It is very much conspicuous from the significant improvement in strength at 900 and 1200 °C, observed from Fig. 6(a) and (b) too, within the same region. Better homogeneity and uniform distribution of particles might be an important factor to get better properties of M-bonded castable. The closer proximity of silica and alumina fines in mullite sol also plays a pivotal role to result in sufficient mullite phases needed for the reinforcement of castable matrix and this is supported from the XRD report of mullite sol at 1200 °C. The sharp increase of CCS value of M-samples between 900 and 1200 °C [Fig. 6(c)] is observed and may be probably due to the enhanced ceramic bonding from the reactive gel phase along with the presence of abundant corundum phases building up the well packed microstructure. No significant improvement in the properties of M-samples at 1500 °C has taken place and might be due to an excess of amorphous material with expansion in local volume. For S-samples at 1500 °C, an improvement of porosity and BD has been observed. It is possibly due to the suspension of α-alumina crystal on cooling which was associated in spinel at higher temperature as solid solution in an excess amount by

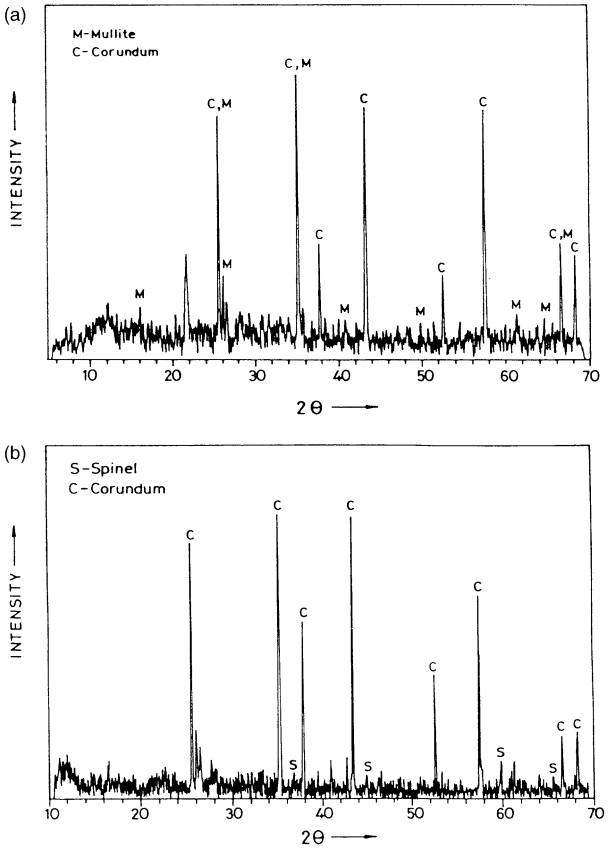

Fig. 8. XRD patterns of sol-bonded ultra low cement castable fired at 1200 °C (a) M type, (b) S type (C = corundum, M = mullite, S = spinel).

widening the spinel lattice. However, the strength of S-samples at 1500 °C was not so satisfactory.

3.2.2. Flexural strength

The flexure (or cold modulus of rupture) test was determined at a temperature of 25 °C with both kind of samples previously fired at 1500 °C. The values of stress at break for M and S samples were found to be 20 and 4 MPa, respectively, which again supported that mullite bonded castables were better than the spinel ones and withstood a greater breaking load due to its better compaction and microstructure.

3.2.3. Thermal shock resistance

Having performed this test as mentioned earlier, residual strength of both kind of castables were compared (Fig. 7). It was interesting to note that S-samples retained almost 95% of its original strength whereas M-samples retained around 80%. As the porosity of S-samples is greater than M-type at all temperatures, we may suggest that the scattered pores in spinel bonded castable tend to prevent the extension of cracks and therefore contribute to improved spalling resistance.

3.2.4. XRD reports

Fig. 8(a) and (b) show the XRD patterns of M and S-type castables fired at 1200 °C respectively. Both the figures show high intensity of corundum peaks that must have appeared as major phases due to the presence of tabular and fused alumina aggregates, which build up the castable skeleton. Apart from these α-alumina phases, it is observed that mullite [Fig. 8(a)] and spinel [Fig. 8(b)] phases have also appeared in the respective castable matrices at 1200 °C. This sort of mullitisation and spinellisation at relatively lower temperatures have taken place due possibly to the reaction of boehmite sol with fumed SiO_2 and $MgCl_2 6{\cdot}H_2O$, respectively.

3.2.5. Slag corrosion resistance

After conducting this test as described earlier, the average slag penetration depth was measured. It was found that for M and S type castable this thickness was 8 and 15 mm, respectively. So obviously mullite sol bonded castables exhibited better slag corrosion resistance. As the compactness for M-samples is higher, we may suggest this to be the reason for its better susceptibility against the slag attack at hot condition. On the

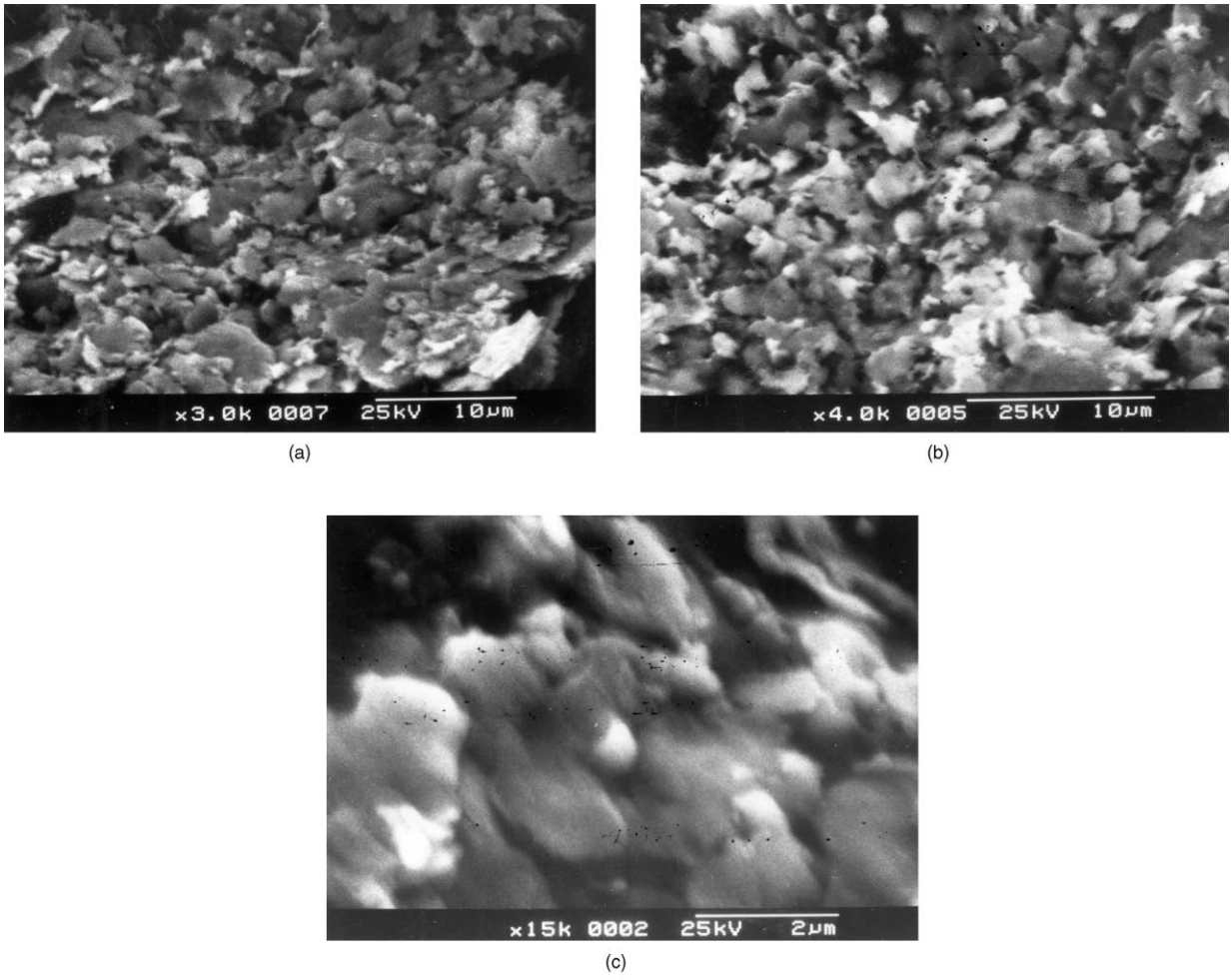

Fig. 9. SEM photographs of M-type ultra low cement castables fired at 1200 °C (a)×3000, (b)×4000 and (c)×15,000.

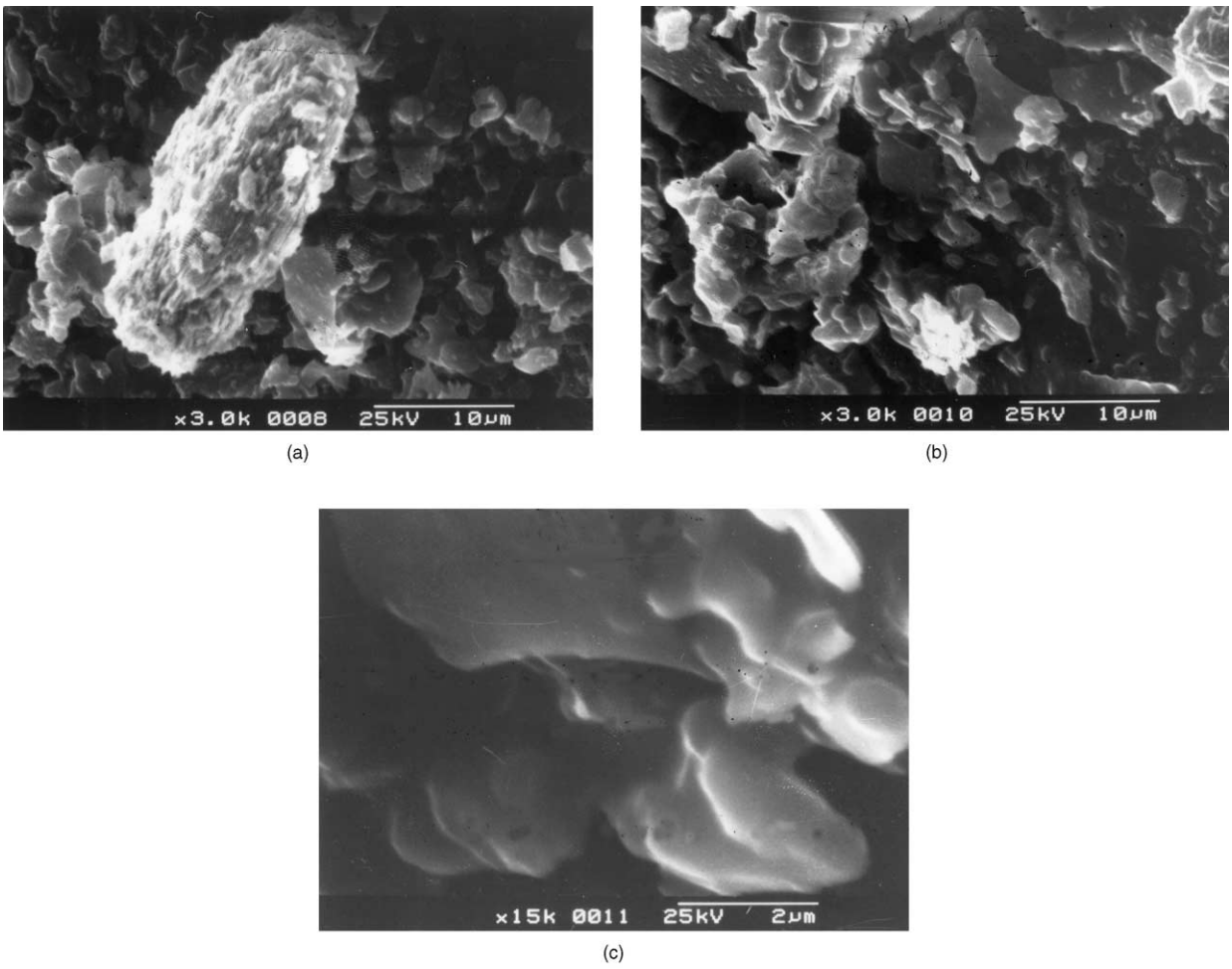

Fig. 10. SEM photographs of S-type ultra low cement castables fired at 1200 °C (a)×3000, (b)×3000 and (c)×15,000.

contrary, the S-samples with poor compaction are more prone to slag attack.

3.2.6. SEM study

Figs. 9 and 10 are the SEM photographs of, respectively, M and S type castables fired at 1200 °C. We may explain the comparative study of BD, AP and CCS of those specimens by drawing analogy to the respective microstructures. Fig. 9(a–c) show densely packed microstructures with an abundant of corundum grains of comparable sizes, rounded and sub-rounded, homogeneously embedded in the matrix. Some needle-shaped mullite crystals too are distributed from place to place, which reinforced the matrix and confirmed the high strength of castables. Very few cracks and voids are visible. An interlocking nature of the uniformly sintered matrix supports the other good qualities of M-type castables. Fig. 10(a–c) show a non-uniform heterogeneous matrix of S-type castables where bonding is disjointed at place to place with locally agglomerated particles and sporadic cracks and voids. Early spinellisation may help large abnormal grains to grow in some regions, due to pore-grain boundary breakaway that deteriorate the mechanical properties. The expansion of spinel bond material may cause the friability of platelets found in different regions. Grain shapes vary from spherical to polyhedral nature and some pores are trapped inside the grains. Gas forming reactions and high chloride concentration may give rise to swelling and fractured surface in some places. An imbalance between lattice and surface diffusion may possibly create a discord in intraagglomerate and interagglomerate sintering which accelerate the rate of coarsening in comparison to densification.

4. Conclusions

From the present study, it may be concluded that the easily prepared mullite sol, when used as an additive in ultra low cement-castable composition, offers a desirable combination of valuable properties. But the spinel sol is not compatible to that composition. It may further be suggested that this mullite-forming route may be exploited here due to the following reasons:

1. Better homogeneity and control of composition is possible to result in an improved castables microstructure.
2. High reactivity with microfines presents in sol saves energy and minimizes air pollution.
3. The rheology of sol enhances the workability of the castable by eliminating expensive and time consuming mixing and vibrating instruments.
4. It is cost effective as less costly precursors are used instead of alkoxides.
5. The shrinkage problem and extended drying period associated with the bulk sol-gel products are minimized here as only 10–13% sol is used in the castable matrix.

Acknowledgements

The authors wish to express their sincere thanks to Dr. A. K. Banerjee, Officer-in-Charge, College of Ceramic Technology, for his help rendered at various stages during the course of experiments. The authors are grateful to Dr. S. K. Das, Refractory Division, Central Glass and Ceramic Research Institute, Kolkata for his valuable suggestions given during this work.

References

[1] S. Banerjee, A Comprehensive Handbook on Monolithic Refractories, The American Ceramic Society, Westerville, OH, USA, 1998.
[2] C.F. Chan, Y.C. Ko, Influence of coarse aggregate content on the thermal conductivity of alumina-spinel castables, J. Am. Ceram. Soc. 79 (11) (1996) 2961–2964.
[3] P. Nandi, L. Tiwari, M.S. Mukhopadhyay, Micronized α-alumina in zero cement castables, Am. Ceram. Soc. Bull. 75 (11) (1996) 71–75.
[4] A.R. Studart, W. Jhong, V.C. Pandolfelli, Rheological design of zero cement self flow castables, Am. Ceram. Soc. Bull. May (1999) 65–72.
[5] S. Mukhopadhyay, S.K. Das, Role of alumina sol on the physical properties of low cement castables, Trans. Ind. Ceram. Soc. 59 (3 part A) (2000) 68–74.
[6] A.Y. Chen, J.D. Cawley, Extrusion of α-alumina-boehmite mixtures, J. Am. Ceram. Soc. 75 (3) (1992) 575–579.
[7] B. Kindle, D.J. Carlsson, Y. Deslandes, A.J. Hoddenbagh, Preparation of α-alumina ceramics: The use of boehmite sol as dispersion agent, Ceramics International 17 (1991) 347–350.
[8] A.C. Pierre, D.R. Uhlmann, Gelation of aluminium hydroxide sols, J. Am. Ceram. Soc. 70 (1) (1987) 28–32.
[9] C. Sunilkumar, U.S. Hareesh, A.D. Damodaran, K.G.K. Warrior, Monohydroxy aluminium oxide as a reactive binder for extrusion of alumina ceramics, J. Eur. Ceram. Soc. 17 (1997) 1167–1172.
[10] S. Kwon, G.L. Messing, Constrained densification in boehmite–alumina mixtures for the fabrication of porous alumina ceramics, J. Mater. Sci. 33 (1998) 913–921.
[11] A.R. Boccaccini, T.K. Khalil, M. Bucker, Activation energy for the mullitization of a diphasic gel obtained from fumed silica and boehmite sol, Mater. Lett. 38 (2) (1999) 116–120.
[12] J.C. Debsikder, Preparation of transparent non-crystalline stoichiometric magnesium-aluminate gel-monolith by the sol–gel process, J. Mater. Sci. 20 (12) (1985) 4454–4458.
[13] S. Mukhopadhyay, S. Dutta, M. Majumdar, A. Kundu, S.K. Das, Synthesis and characterization of alumina bearing sol for application in refractory castables, Industrial Ceramics 20 (2 September) (2000) 88–92.
[14] T. Ban, S. Hayashi, A. Yasumori, K. Okada, Characterization of low temperature mullitization, J. Eur. Ceram. Soc. 16 (1996) 127–132.
[15] D.J. Janackovic, V. Jokanovic, I. Petrovic-Prelevic, D. Uskokovic, Synthesis of spinel powders by the spray pyrolysis method, Euro Ceramics V (part I) (1997) 197–200.
[16] S. Mukhopadhyay, S. Mahapatra, P. Mukherjee, T. Dasgupta, S.K. Das, Effect of alumina sol in no cement refractory castables, Trans. Ind. Ceram. Soc. 60 (2) (2001) 63–67.
[17] J.S. Reed, Introduction to the Principles of Ceramic Processing, John Wiley, New York, 1989 (Chapter 15).
[18] C. Kaya, P.A. Trusty, C.B. Ponton, Characterization of nano-sized colloidal suspensions for the preparation of multilayer alumina fibre-reinforced mullite CMC & using electrophoretic filtration deposition (EFD), in: J. Binner, J. Yeomans (Eds.), British Ceramic Proceedings, no.58, Better Ceramics Through Processing, IOM Communications Ltd, London, UK, 1998, pp. 93–101.
[19] Sang H. Hyun, Seung R. Song, Low-temperature synthesis of mullite powders by the emulsion route, J. Mater. Sci. Lett. 13 (3) (1994) 177–179.
[20] J.C. Huling, G.L. Messing, Chemistry-crystallization relations in molecular mullite gels, J. Non-Cryst. Solids 147 & 148 (1992) 213–221.
[21] D.J. Cassidy, J.L. Woolfrey, B. Ben-Nissan, J.R. Bartlett, The effect of precursor chemistry on the crystallization and densification of sol–gel derived mullite gel and powders, J. Sol–Gel Sci. Technol. 10 (1) (1997) 19–30.
[22] A.K. Bhattacharya, A. Hartridge, K.K. Mallick, Inorganic aluminium precursors in the synthesis of mullite—an investigation, J. Mater. Sci. 31 (20) (1996) 5551–5554.
[23] K. Wang, M.D. Sacks, Mullite formation by endothermic reaction of α-alumina/silica microcomposite particles, J. Am. Ceram. Soc. 79 (1) (1996) 12–16.
[24] A.K. Chakraborty, Role of hydrolysis water-alcohol mixture on mullitization of Al_2O_3–SiO_2 monophasic gels, J. Mater. Sci. 29 (23) (1994) 6131–6138.
[25] J. Temuujin, K. Okada, Kenneth J.D. Mackenzie, Effect of mechanochemical treatment on the crystallization behavior of diphasic mullite gel, Ceramics International 25 (1) (1999) 85.
[26] P. Padmaja, G.M. Anilkumar, P. Krishna Pillai, A.D. Damodaran, K.G.K. Warrior, Formation characteristics and densification behavior of diphasic mullite gels under various pH conditions, Brit. Ceram. Trans. 97 (5) (1998) 232–235.
[27] L. Pach, A. Iratni, V. Kovar, P. Mankos, S. Komarneni, Sintering of diphasic mullite gel, J. Eur. Ceram. Soc. 16 (5) (1996) 561–566.
[28] A. Goldstein, L. Giefman, S. Bar Ziv, Susceptor assisted microwave sintering of $MgAl_2O_4$ powder at 2.45 GHz, J. Mater. Sci. Lett. 17 (12) (1998) 977–979.
[29] I. Lazau, C. Pacurariu, D. Becherescu, Aspects regarding the formation of the spinel phase in the MeO–Al_2O_3 and MeO–TiO_2 system, Euro Ceramics V (part-I) (1997) 65–68.
[30] G. Lallemand, S. Fayeulle, D. Treheux, Fabrication process of spinel powder for plasma spraying, J. Eur. Ceram. Soc. 18 (14) (1998) 2095–2100.
[31] Ching-Jui. Ting, Hong-Yang. Lu, Defect reactions and the controlling mechanism in the sintering of magnesium aluminate spinel, J. Am. Ceram. Soc. 82 (4) (1999) 841–848.

[32] G. Gusmano, P. Nunziante, E. Traversa, G. Chiozzini, The mechanism of $MgAl_2O_4$ spinel formation from the thermal decomposition of co-precipitated hydroxides, J. Eur. Ceram. Soc. 7 (1991) 31–39.
[33] V.K. Singh, R.K. Sinha, Low temperature synthesis of spinel ($MgAl_2O_4$), Mater. Lett. 31 (3–6) (1997) 281–285.
[34] Y. Suyama, A. Kato, Characterization and sintering of Mg–Al spinel prepared by spray-pyrolysis technique, Ceramics International 8 (1) (1982) 17–21.
[35] R.J. Bratton, Coprecipitates yielding $MgAl_2O_4$ spinel powders, Am. Ceram. Soc. Bull. 48 (8) (1969) 759–762.
[36] E. Ryshkewitch, Oxide Ceramics, Academic Press, New York, 1960.